Available online at www.sciencedirect.com

SciVerse ScienceDirect

Ceramics International 39 (2013) 1221–1225

CERAMICS INTERNATIONAL

www.elsevier.com/locate/ceramint

Preparation of $Ni_{1-x}Mn_xFe_2O_4$ ferrites by sol–gel method and study of their cation distribution

Abid Hussain[a,*], Tahir Abbas[a], Shahida B. Niazi[b]

[a]Department of Physics, Bahauddin Zakariya University, Multan 60800, Pakistan
[b]Department of Chemistry, Bahauddin Zakariya University, Multan 60800, Pakistan

Received 6 June 2012; received in revised form 16 July 2012; accepted 16 July 2012
Available online 23 July 2012

Abstract

The spinel ferrite nanoparticles of the system $Ni_{1-x}Mn_xFe_2O_4$ with $x=0.0$, 0.1, 0.3, 0.5, 0.7 and 0.9 were prepared by sol–gel auto combustion technique using chlorides of Ni, Mn and Fe as a source with citric acid as chelating agent. The structure of the ferrite materials and the particle size were determined by XRD, it was observed that the structure was a single phase, face centered cubic with lattice parameter ranging from 8.365 Å to 8.394 Å and the particle size ranging from 23.86 Å to 38.30 Å. The lattice parameter showed a linear dependence on concentration in accordance with the Vegard's law. By analyzing XRD patterns, the cation distribution over *A* and *B*-sites was estimated through the R-Factor method. The magnetic moment for each sample was determined from cation distribution on the two sites. An enhancement in the net magnetic moment was observed with gradual increase in the Mn content.
© 2012 Elsevier Ltd and Techna Group S.r.l. All rights reserved.

Keywords: Ferrites; Sol–gel auto combustion technique; Chelating agent; Cation distribution

1. Introduction

Chemically prepared magnetic nanoparticles exhibit superior magnetic properties compared to their bulk counterparts due to small particle size and uniform distribution. Technically, spinel ferrites are an important group of magnetic materials with diverse properties applicable in the fabrication of electronic, magnetic and microwave devices. Nickel ferrites find applications in low as well as in high frequency devices due to high electrical resistivity, high mechanical hardness and good chemical stability. They are mostly used in magnetic recordings, telecommunication, power transformers, storage devices and drug delivery systems [1].

The unit cell of the spinel ferrite is formed by doubling the face centered cubic oxygen sublattice along each of the three dimensions. In this arrangement 64 tetrahedral or *A*-sites and 32 octahedral or *B*-sites are created in the unit cell. In stoichiometric spinels only 8 *A*-sites and 16 *B*-sites are filled by divalent transition-metal ions. The spinel compounds belong to the space group Fd3m ($F^4_{1/d}\bar{3}_{2/m}$, No. 227 in the International Tables for X-ray Crystallography) with lattice parameter 8.5 Å. In mixed spinel ferrites the concentrations of ferrous, ferric and substituted metal ions and their distribution over tetrahedral and octahedral sites play a vital role in determining their magnetic and electrical properties. In normal spinels, all the *A*-sites are occupied by divalent transition metal ions while in inverse spinels; the divalent ions occupy *B*-sites. In disordered spinels the divalent ions are present on both *A* and *B*-sites. The normal and inverse spinels are two extremes between which the cation distribution may vary. When the origin of the unit cell is taken at the centers of symmetry $\bar{4}3m$ and $\bar{3}m$, then oxygen positional parameter *u* (the distance between the oxygen ion and the face of the cube edge along the cube diagonal of the spinel subcell) has ideal values 0.375(3/8) and 0.250(1/4) respectively, for a perfect cubic close-packed arrangement of oxygen ions. In this case the octahedral cation–anion distance or bond length is 1.155 times larger than the tetrahedral bond length. A deviation from the ideal structure occurs when oxygen is displaced along [111] direction to accommodate the constituent cations, the tetrahedral site with smaller

*Corresponding author. Tel.: +92 61 9210091; fax: +92 61 9210098.
E-mail address: ahussainbzu@gmail.com (A. Hussain).

0272-8842/$ - see front matter © 2012 Elsevier Ltd and Techna Group S.r.l. All rights reserved.
http://dx.doi.org/10.1016/j.ceramint.2012.07.049

volume enlarges at the expense of the octahedral site and then u has a value greater than 0.375.

In order to control the domain of ferrite's applications, the investigation of cation distribution on A and B-sites and oxygen positional parameter u, is most important [2].

To determine the cation distribution in spinels many techniques have been employed so far, some of them are neutron diffraction [3], thermoelectric measurements [4], electron spin resonance [5] etc. Analyzing the X-ray diffraction patterns cation distribution can be estimated by several methods, like the Bertaut method [6], the Furuhashi method [7], and the R-Factor method [8]. Investigations on the cation distribution for $NiFe_2O_4$ [9], $NiMn_xFe_{2-x}O_4$ [10] and $Ni_xMn_{1-x}Fe_2O_4$ [11] have been reported. In the present work, the R-Factor method has been employed to estimate the cation distribution and to calculate the oxygen positional parameter in $Ni_{1-x}Mn_xFe_2O_4$ ferrites.

2. Experimental procedures

2.1. Preparation of samples

The nanoparticle powders of $Ni_{1-x}Mn_xFe_2O_4$ with $x=0.0$, 0.1, 0.3, 0.5, 0.7, and 0.9 were prepared using the sol–gel auto combustion method from reagent grade constituents; nickel chloride, manganese chloride and ferric chloride provided by Merck Germany. The ferrite powders were obtained through a procedure described below.

2.1.1. Sol-formation

The stoichiometric amount of metal chlorides and citric acid was dissolved into de-ionized water to form a mixed solution. Homogenous distribution and segregation of the metal ions was achieved by the use of citric acid. The pH value of the solution was maintained in the range 7–8 by drop wise addition of ammonia solution (base catalyst) in order to speed up the reaction. The solution was constantly stirred using a magnetic agitator. The condensation reaction took place between the adjoining metal chlorides and the molecules of citrates yielding a polymer precursor in colloidal dimensions known as sol.

2.1.2. Gel formation

The obtained sol was heated at 80 °C on a hot plate under regular stirring to condensate into a xerogel.

2.1.3. Powder formation

An increase of temperature upto 250 °C led to the ignition of the dry gel and a loose ferrite nanopowder was obtained through the burning of gel in a self-propagating combustion manner. During the combustion process, exothermic decomposition of a redox mixture of metal chlorides and citric acid took place along with the removal of gases such as Cl_2, CO, H_2O, and CO_2.

2.1.4. Annealing

The prepared powder samples were then annealed for 5 h at 500 °C in order to enhance the crystallinity.

2.1.5. Characterization

The annealed powders were characterized by powder X-ray diffraction technique using an X-ray diffractometer Shimadzu XD-5 A at room temperature with Cu Kα source radiation of wavelength $\lambda=1.540$ Å. The phase constitution and structure of each composition were determined by indexing the XRD patterns.

2.2. Site preference analysis

The R-Factor method was used to determine the values of the inversion parameter δ and oxygen positional parameter u in Ni–Mn ferrites. This method works well for the selection of the best fit simulated structure by minimizing the value of the residual function R. For this purpose a computer program in FORTRAN-77 was developed. The program was run for 10–100 iterations. The values of δ, u and R for each composition were recorded to justify the site occupancies. Two of the several expressions used for the residual function R are as follows:

$$R_1 = \frac{\sum_{hkl}\left|I_{obs}^{hkl}-I_{cal}^{hkl}\right|}{\sum_{hkl}I_{obs}^{hkl}} \quad (1)$$

$$R_2 = \frac{\sum_{hkl}\left|\sqrt{I_{obs}^{hkl}}-\sqrt{I_{cal}^{hkl}}\right|}{\sum_{hkl}\sqrt{I_{obs}^{hkl}}} \quad (2)$$

where I_{obs}^{hkl} and I_{cal}^{hkl} are the observed and calculated intensities for hkl reflection respectively. For the computation of the relative integrated intensity of a given diffraction line, the following formula is applicable.

$$I_{\mathrm{hkl}} = |F|^2 P L_{\mathrm{P}}$$

where F is the structure factor, P is the multiplicity factor and L_P is the Lorentz-polarization factor.

3. Results and discussion

3.1. Phase analysis and particle size of ferrite powders

The X-ray diffraction lines in Fig. 1 provided a clear evidence of the formation of a pseudo solid solution of the $Ni_{1-x}Mn_xFe_2O_4$ ferrites. Mean value of the lattice parameter a calculated from main diffraction peak of each sample indicated a linear Mn content dependence as shown in Fig. 2. Since the ionic radius of Mn^{2+} (Tet: 0.655 Å; Oct: 0.80 Å) is greater than that of Ni^{2+} (Tet: 0.55 Å; Oct: 0.69 Å) [11], the replacement of nickel ion by manganese ion caused an increase in the interatomic spacing parameter d and consequently lattice parameter increased in accordance with the Vegard's law [12]. The value of lattice parameter for the $NiFe_2O_4$ was found to be $a=8.365$ Å,

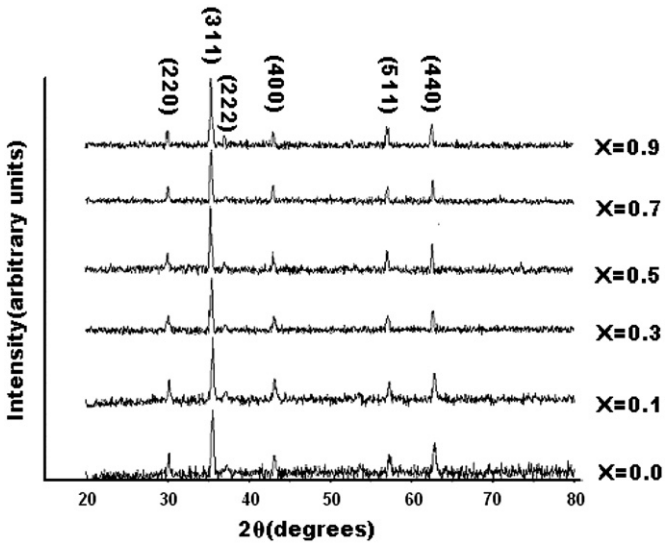

Fig. 1. X-ray diffraction patterns of the $Ni_{1-x}Mn_xFe_2O_4$ system.

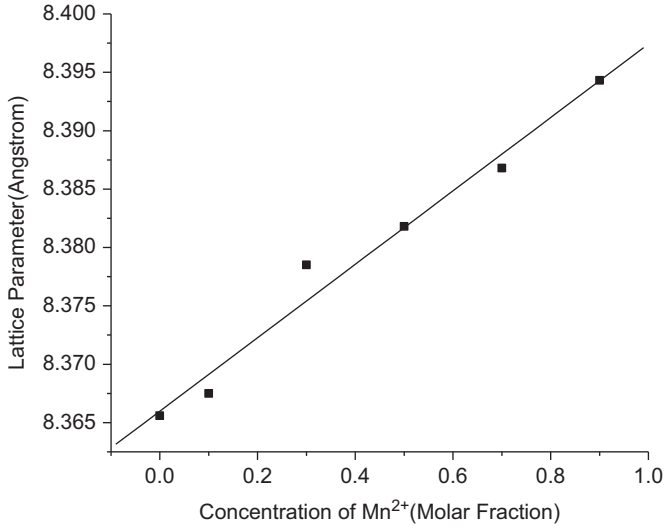

Fig. 2. Lattice parameter as a function of Mn content in $Ni_{1-x}Mn_xFe_2O_4$.

which was in good agreement with that obtained from JCPDS card (10325), for nickel iron oxide i.e. $a=8.339$ Å. The particle size of the powders was determined by the Scherrer's equation [13] as follows:

$$D_{hkl} = \frac{0.9\lambda}{B_{hkl}\cos\theta}$$

Here D_{hkl} was the particle size obtained from the peak with maximum intensity which corresponded to the Miller indices (311) in all XRD patterns. B_{hkl} was full width of the peak at half maximum (in radians). The particle size against each composition was shown in Table 1.

The change in particle size was attributed to the ionic radii of the constituent metals [14]. The crystallites were more compact in the sample with $x=0.0$, as Ni^{2+} ion was smaller one and could dissolve in the spinel lattice shown in Fig. 3, substitution of Mn^{2+} ion caused an increase in porosity of grains due to its greater ionic radius and the grains were less compact causing an increase in particle size.

3.2. Estimation of cation distribution

By inputting the data obtained from XRD patterns and fractional coordinates of lattice sites in a spinel cubic unit cell as listed in Table 2 [15], the inversion parameter δ and oxygen positional parameter u were calculated from the computer program in FORTRAN-77 by minimizing the value of the residual function R.

The general formula used for cation distribution in $Ni_{1-x}Mn_xFe_2O_4$ ferrites was expressed as

$$Me^{3+}_{1-\delta}Me^{2+}_{\delta}[Me^{3+}_{1+\delta}Me^{2+}_{1-\delta}]O_4$$

The brackets were used to represent the cations at octahedral sites. Inversion parameter δ, oxygen positional parameter u and residual function R for $Ni_{1-x}Mn_xFe_2O_4$ are listed in Table 3. The cation distribution for $Ni_{1-x}Mn_xFe_2O_4$ is listed in Table 4.

According to our results a gradual increase in inversion parameter with x indicated that nickel ferrite was an

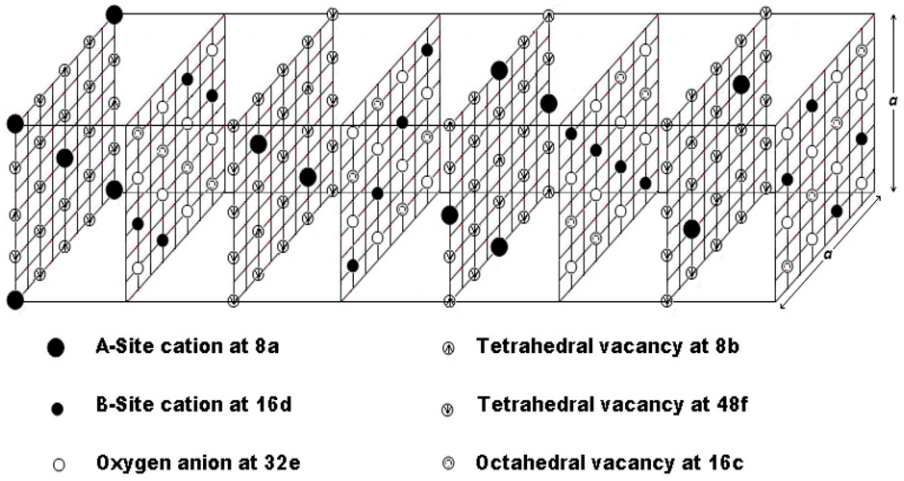

Fig. 3. Spinel lattice sites in a cubic cell, layers are shown at ***a*/8** interval along [100] cubic cell axis.

Table 1
Particle size in $Ni_{1-x}Mn_xFe_2O_4$.

Composition (x)	0.0	0.1	0.3	0.5	0.7	0.9
Particle size (nm)	23.86	26.47	30.33	31.64	33.85	38.30

Table 2
Fractional coordinates of lattice sites in a spinel cubic unit cell.

Lattice sites	Equipoint	Point symmetry	Fractional coordinates of lattice sites
			Origin on $\bar{4}3$ m at A-site cation (1/8,1/8,1/8 from $\bar{3}$ m on octahedral vacancy) (0,0,0; 0,1/2,1/2; 1/2,0,1/2; 1/2,1/2,0)+
A-site cation	8a	$\bar{4}3m$	0,0,0; 1/4,1/4,1/4
Tetrahedral vacancy	8b	$\bar{4}3m$	1/2,1/2,1/2; 3/4,3/4,3/4
B-site cation	16d	$\bar{3}m$	5/8,5/8,5/8; 5/8,7/8,7/8; 7/8,5/8,7/8; 7/8,7/8,5/8
Octahedral vacancy	16c	$\bar{3}m$	1/8,1/8,1/8; 1/8,3/8,3/8;3/8,1/8,3/8; 3/8,3/8,1/8
Anion	32e	3m	u,u,u; u,$\bar{u}$, $\bar{u}$;$\bar{u}$,u,$\bar{u}$;$\bar{u}$,$\bar{u}$,u; (1/4−u),(1/4−u),(1/4−u); (1/4+u),(1/4+u),(1/4−u); (1/4+u),(1/4−u),(1/4+u); (1/4−u),(1/4+u),(1/4+u)
Tetrahedral vacancy	48f	mm	1/4,0,0; 0,1/4,0; 0,0,−1/4; −1/4,0,0; 0,−1/4,0; 0,0,−1/4; 1/2,1/4,1/4; 1/4,1/2,1/4; 1/4,1/4,1/2; 0,1/4,1/4; 1/4,1/4,0; 1/4,0,1/4

Table 3
Inversion parameter δ, oxygen positional parameter u and residual function R for $Ni_{1-x}Mn_xFe_2O_4$.

x	δ	u	R
0.0	0.1	0.377	0.064
0.1	0.1	0.378	0.066
0.3	0.2	0.380	0.071
0.5	0.3	0.380	0.065
0.7	0.4	0.381	0.082
0.9	0.5	0.381	0.056

inverse spinel and manganese ferrite was normal spinel. It was deduced that lattice parameter and oxygen positional parameter were directly related to the degree of inversion.

3.3. Calculation of magnetic moment

The magnetic moments of A-site cations and B-site cations oppose each other in an applied magnetic field [16]. The ionic magnetic moments for ions of 3d transition elements Fe^{3+}, $Ni^{2+}$and $Mn^{2+}$are 5 μ_B, 2 μ_B and 5 μ_B respectively [16]. The distribution of cations on the two sites in spinels determines the net magnetic moment of the formula unit. In our work, the induction of Mn^{2+} ions in $Ni_{1-x}Mn_xFe_2O_4$ ferrites caused a migration of Fe^{3+} ions from A-site to B-site, hence there was more imbalance in spins between the two sites, consequently the magnetization at B-site (M_B) was increased; and A–B interaction gave the net magnetic moment, as shown in Table 5.

Table 4
Cation distribution in $Ni_{1-x}Mn_xFe_2O_4$.

Concentration (x)	Distribution of cations					
	Tetrahedral site (A)			Octahedral site (B)		
	Ni^{2+}	Mn^{2+}	Fe^{3+}	Ni^{2+}	Mn^{2+}	Fe^{3+}
0.0	0.1	0.0	0.9	0.9	0.0	1.1
0.1	0.09	0.01	0.9	0.81	0.09	1.1
0.3	0.14	0.06	0.8	0.56	0.24	1.2
0.5	0.15	0.15	0.7	0.35	0.35	1.3
0.7	0.12	0.28	0.6	0.18	0.42	1.4
0.9	0.05	0.45	0.5	0.05	0.45	1.5

Table 5
Magnetic moment for $Ni_{1-x}Mn_xFe_2O_4$.

Concentration (x)	0.0	0.1	0.3	0.5	0.7	0.9
Magnetic moment (μ_B)	2.6	2.84	3.74	4.4	4.82	5.0

4. Conclusion

The $Ni_{1-x}Mn_xFe_2O_4$ nanoparticles can be prepared using the sol–gel technique. The phase identification and estimation of cation distribution were possible to carry out on the basis of XRD data. The values of inversion parameter and oxygen positional parameter indicated that the ferrites system belonged to a family of mixed or partially inverse spinels. It was observed that particle size in the ferrites tended to increase as the degree of inversion increased. The relationship among structural parameters (a, u) and the inversion parameter (δ) was studied and found that the lattice parameter was dependent on the average effective cation radius in the compound and had no significant dependence on the arrangement of cations; however the oxygen parameter was dependent on the distribution of cations.

Acknowledgment

The authors appreciate the financial support from the Higher Education Commission of Pakistan.

References

[1] M.K. Shobana, S. Sankar, V. Rajendran, Structural and thermal studies of $Ni_{0.25}Mn_{0.75}Fe_2O_4$ composites by sol–gel combustion method, Journal of Alloys and Compounds 472 (2009) 421–424.

[2] Tahir Abbas, Y. Khan, Mushtaq Ahmed, Shahid Anwar, X-ray diffraction study of the cation distribution in the Mn–Zn ferrites, Solid State Communications 82 (1992) 701–703.
[3] E. Stall, P. Fischer, W. Halg, G. Maier, Redetermination of the cation distribution of spinel ($MgAl_2O_4$) by means of neutron diffraction, Journal of Physics (Paris) 25 (1964) 447–448.
[4] C.C. Wu, T.O. Mason, Thermopower measurement of cation distribution in magnetite, Journal of American Ceramic Society 64 (1981) 520–522.
[5] U. Schmocker, H.R. Boesch, F. Waldner, A direct determination of cation disorder in $MgAl_2O_4$ spinel by ESR, Physics Letters 40A (1978) 237–238.
[6] J.M. Rubio Gonzalez, C.O. Arean, X-ray diffraction determination of the cation distribution and oxygen positional parameter in polycrystalline spinels, Journal of the Chemical Society, Dalton Transactions (1985) 2155–2159.
[7] H. Furuhasi, M. Inagaki, S. Naka, Cation distribution in the solid solution of the $CoAl_2O_4$, $GeCo_2O_4$ system, Journal of Inorganic and Nuclear Chemistry 35 (1973) 3009.
[8] Mazhar U Rana, M.U. Islam, Tahir Abbas, Cation distribution in Cu substituted Mn ferrites, Journal of Materials Letters 41 (1999) 52–56.
[9] S.T. Hugh, C. O Neill, A. Navrotsky, Simple spinels: crystallographic parameters, cation radii, lattice energies, and cation distribution, American Mineralogist 68 (1983) 181–194.
[10] Qiang-min Wei, Jian-biao Li, Yong-jun Chen, Yong-Sheng Han, X-ray study of cation distribution in $NiMn_{1-x}Fe_{2-x}$ ferrites, Journal of Materials Characterization 47 (2001) 247–252.
[11] Qiang-min Wei, Jian Biao Li, Yong Junchen, Cation distribution and infrared properties of Ni_xMn_{1-x} ferrites, Journal of Materials Science 36 (2001) 5115–5118.
[12] B.D. Cullity, Elements of X-rays Diffraction (1977) Indiana.
[13] S.M. Attia, Study of cation distribution of Mn–Zn ferrites, Egyptian Journal of Solids 29 (2) (2006).
[14] Yu. Zhong, L.A.N. Zhongwen, Cheng Shengming, Microstructure and magnetic properties of Ni substituted high density MnZn ferrites, Rare Metals 25 (2006) 584–587.
[15] K.E. Sickafus, J.M. Wills, Structure of spinel, Journal of American Ceramic Society 82 (1999) 3279–3292.
[16] W.S. Smith, Principles of Material Science and Engineering, McGraw-Hill, 1990.